Development of a Compact Planar Multiband MIMO Antenna for 4G/LTE/WLAN Mobile Phone Standards

Foez Ahmed*, Ronglin Li†, *Senior Member, IEEE*, and Ying Feng*, *Member, IEEE*
*School of Automation Science and Engineering
†School of Electronic and Information Engineering
South China University of Technology, Guangzhou, China-510640
Email: foez28@ru.ac.bd, lirl@scut.edu.cn, yfeng@scut.edu.cn

***Abstract*-A compact planar multiband MIMO antenna system is developed. The MIMO antenna consists of two symmetric antenna elements, each of which comprises three effective radiators: a driven monopole, a meandered S- and F-shaped strip and all are printed on the front side of a thin low-cost substrate. At VSWR ≤ 2.75, the proposed MIMO antenna operates in the frequency range of LTE-1, LTE-2, LTE-3, LTE-7, LTE-40, and WLAN 2.4 GHz bands. The experimental results verify the simulations. Higher isolation (> 18 dB) is achieved. The received signals satisfy the condition $P_i \approx P_j$. The measured correlation coefficient is lower than 0.01 and radiation patterns of each antenna unit can cover complementary space region that confirms both the spatial and pattern diversity.**

Keywords – MIMO antenna, Broadband, LTE, Handsets

I. INTRODUCTION

Doubtless that the modern wireless communication system demands reliable transmission with higher - data rate, channel capacity and spectral efficiency in a rich scattering environment. But the channel capacity of a conventional single-input single-output (SISO) communication system is limited according to the Shannon's theorem [1]. The Long Term Evolution (LTE) standard for mobile broadband inclusion of Multiple Input Multiple Output (MIMO) transmission technique confirms the improved performance in terms of coverage, spectral efficiency and high data rate without additional power requirements [2][3]. However, the multiband MIMO antenna design for mobile handset is more challenging in many aspects unlike other applications due to its limited space and compactness.

Over the last decade, a significant research has been carried out to design broadband MIMO antenna for mobile handsets. In [4], a printed diversity monopole antenna is presented for WiFi/WiMAX (2.4-4.2 GHz) applications. The achieved isolation is greater than 17 dB. The author of [5] has also studied MIMO antenna for WLAN (2400-2484 MHz) and WiMAX (2500-2690 MHz) applications. The proposed antenna has total system size of $100\times50\times0.8mm^3$ and isolation is roughly 15 dB. In [6], another wideband MIMO antenna has been presented to cover a wideband frequency of 2.4-6.55 GHz with high isolation (>18 dB). A very recent work, proposed by [7] covers a wide band frequency range of 1700-2900 MHz. The total system size is about of $55\times99\times1.6$ mm^3 and isolation is better than 15 dB. Though the antenna has overall better performance but the structure is not fit for farther 3/4-element antenna array systems into the limited volume of mobile handset without compromising system's size. However, in this paper a planar compact wideband MIMO antenna has been presented for future wireless applications of LTE#1 (1920-2170 MHz), LTE#2 (1850-1990 MHz), LTE#3 (1710-1880 MHz), LTE#7 (2500-2690 MHz), LTE#40 (2300-2400 MHz), and WLAN (2400-2484 MHz) bands. The total systems size is $60\times110\times0.8mm^3$ that is a typical handset's size for practical usage as well as comparable with the IPhone4 mobile handset.

II. MIMO ANTENNA DESIGN AND MEASUREMENTS

A. Antenna Structure

The optimized layout with dimensional details of the proposed multiband MIMO antenna is illustrated in Fig. 1. A single antenna unit comprises of a driven monopole (orange colored), an S-shaped strip (blue colored) and F-shaped strip (red colored). The S-strip is short circuited to the ground plane though Via (H). Both of the S- and F-shaped strips are capacitively coupled to each other as well as electromagnetically coupled to the driven monopole. The driven monopole is fed with a 50Ω microstrip line whereas other radiators are coupled-fed. The antenna arrays are printed on the front side of a low cost FR-4 substrate. On the back side of the substrate a system ground plane of size $60\times95mm^2$ is printed. Due to minimizing mutual coupling effects, a protruded T-shaped metal strip with rectangular cutting slots, and two symmetric ground slots have been introduced. The antenna was analyzed using Ansoft HFSS v13 and optimized values are listed in Table I.

A prototype of proposed MIMO antenna is viewed in Fig. 2. The antenna was fabricated on a FR-4 substrate (ε_r=4.6, thickness = 0.8mm, tan(δ) = 0.02) of dimension $110x60mm^2$. The measured VSWR of proposed MIMO antenna is compared with the simulation results in Fig. 3. At VSWR ≤ 2.75, the achieved bandwidths are around 27.4% (1.67-2.2 MHz) and 25.6% (2.28-2.95 GHz).

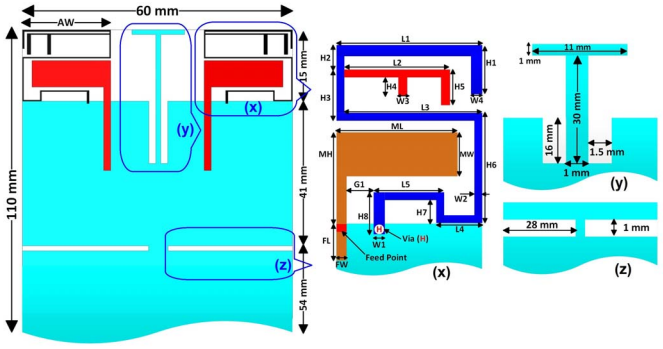

(a) Full Structure (b) Optimized Values

Figure 1. Optimized Geometry details of the proposed 2×2 MIMO antenna

TABLE I
OPTIMIZED PARAMETERS & VALUES (UNIT: MILLIMETERS)

Parameter	Value	Parameter	Value	Parameter	Value
MH	8.5	ML	16.5	MW	5.5
FL	17.5	FW	1.45	G1	0.6
H1	4	H2	0.8	H3	5.2
H4	4.15	H5	4.4	H6	9.25
H7	2.25	H8	2.75	L1	18.5
L2	17.25	L3	18.5	L4	4
L5	10.25	W1	0.5	W2	0.25
W3	0.75	W4	0.04	AW	18.5

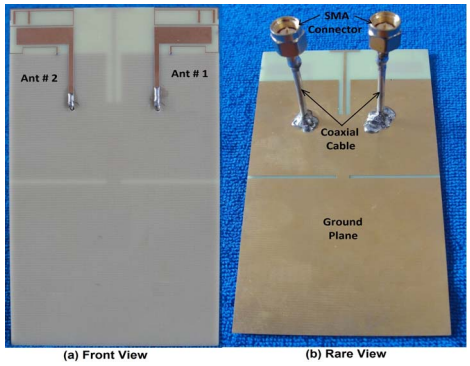

Figure 2. Prototype of the proposed multiband MIMO antenna

B. *Operating Principle and Parameter Study*

The fundamental operating principles are analyzed with the aid of simulated return loss shown in Fig. 4. The corresponding dimension of Ref. 1, Ref. 2, and Ref. 3 are fixed as the optimized values listed in Table I. In case of driven monopole only (Ref. 1), a wide resonant mode is observed at around 2.8 GHz. The length of the driven monopole is about 25mm up to feed point (A) that can excite a quarter-wavelength (λ/4) resonant mode. The length of the S-shaped strip is around 75mm that can excite a half-wavelength (λ/2) resonant mode. Farther by adding F-shaped coupled strip (Ref. 3), a 3rd resonant mode is formed at around 1.83 MHz and the impedance of the 2nd resonant mode is improved. The length of F-shaped strip itself is about 20mm, but with the partial S-shaped strip the total length is about 67mm that generates a half-wavelength (λ/2) resonant mode at 1.83 GHz. The reason behind of exciting (λ/2) resonant mode is that both the S- and F-shaped strips are electromagnetically coupled with the driven monopole.

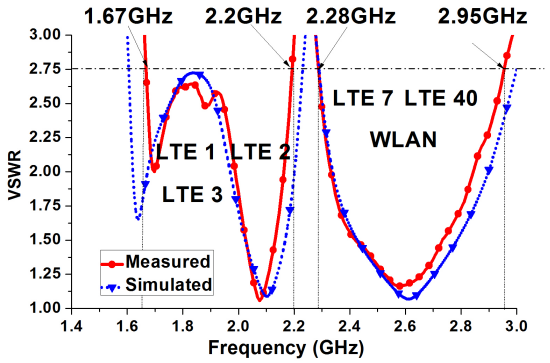

Figure 3. Measured and Simulated results for VSWR characteristics

Unlike direct feeding, couple-fed generally decreases the input impedance and hence lengthens the electrical length of the radiator [8]. Moreover, F-strip is farther capacitively coupled with the S-shaped strip and hence the inductive reactance is compensated by the coupling capacitance introduced by the small gap between the S- and F-shaped strip which extends the length of F-strip electrically and hence excites the 3rd resonant mode [6].

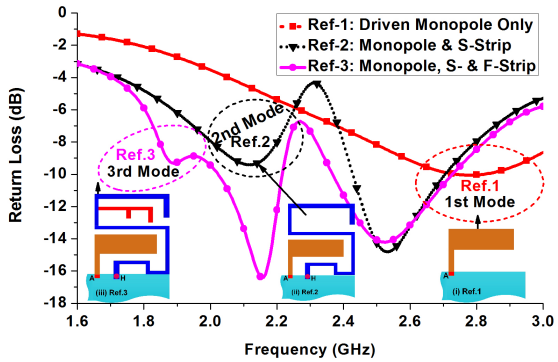

Figure 4. Simulated Return Loss for the case of (i) Driven Monopole only (Ref. 1), (ii) S-shaped Strip with Monopole (Ref. 2), and (iii) F-shaped Strip with S-strip & Monopole (Ref. 3)

Fig. 5 shows the simulated return loss with varying length of H1 while other values are fixed as listed in Table I. As H1 (hence the length of S-strip) is decreased, the 2nd resonant frequency is shifted towards the higher frequency or vice-versa without having any effect on other two resonant modes. In Fig. 6, it is evident that the 3rd resonant frequency is shifted towards the higher frequency as H5 (hence the length of F-strip) is decreased or vice-versa with having minor effect on other two resonant modes. Therefore, it is inferred that radiation characteristic within the 2nd and 3rd resonant modes over the operating bands are controlled and contributed by the S- and F-shaped strip respectively.

C. *Isolation and Decoupling Technique Analysis*

As a decoupling technique, two symmetric rectangular slots and a protruded T-shaped strip with rectangular slots have been studied into the ground plane. In principle, its function is to provide anti-phase coupling currents to eliminate the original

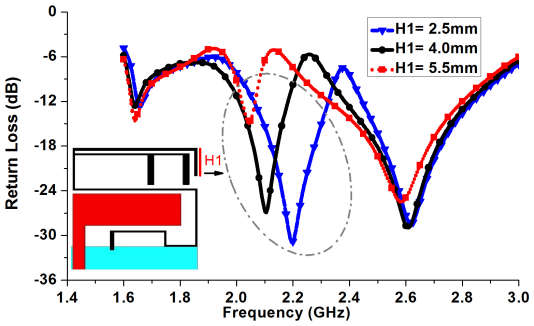

Figure 5. Effect of the length (H1) of S-Strip on the return loss of the proposed MIMO antenna, where H1= 4mm is an optimized value

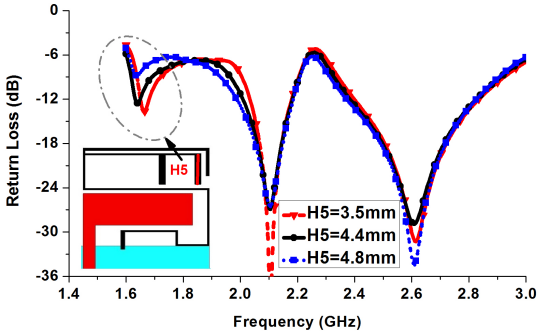

Figure 6. Effect of the length (H5) of F-Strip on the return loss of the proposed MIMO antenna, where H5= 4.4mm is an optimized value

coupling currents. Whereas the cutting slots reduce the mutual coupling effects caused by distributed ground surface currents. The ground slots act as a band stop filter and also make slow the surface currents flow over the finite ground. Surface current distribution shown in Fig. 7 demonstrates the effectiveness of the applied techniques as well. However, the measured isolation curves for the proposed MIMO antenna are compared with the simulation results and plotted in Fig. 8. It is observed that the isolation is greater than 18 dB over the operating bands.

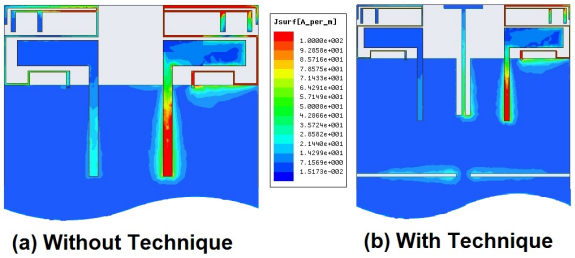

Figure 7. Surface current distribution of 2×2 MIMO antenna at 2GHz (a) Without decoupling techniques and (b) With decoupling techniques

III. Antenna Performance Evaluation

A. *Envelope Correlation Coefficient (ρe)*

In the case of isotropic/uniform signal propagation environment, the envelope correlation coefficient (ρ_{ij}) can be

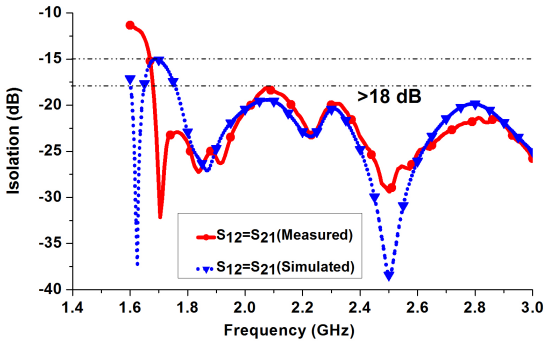

Figure 8. Isolation comparison of the proposed multiband MIMO antenna

computed by Eq. (1) [9],

$$\rho_{ij}^{es} = \left| \frac{\left| S_{ii}^{*} S_{ij} + S_{ij}^{*} S_{jj} \right|}{\sqrt{\left(1 - \left|S_{ii}\right|^2 - \left|S_{ji}\right|^2\right) \times \left(1 - \left|S_{jj}\right|^2 - \left|S_{ij}\right|^2\right)}} \right|^2 \quad (1)$$

The simulated and computed envelope correlation coefficients obtained from measured S-parameter values are plotted in Fig. 9. It is observed that in any of two antenna elements combinations the measured ρ_e the proposed MIMO antenna are always below 0.01, which leads to a perfect performance in terms of diversity.

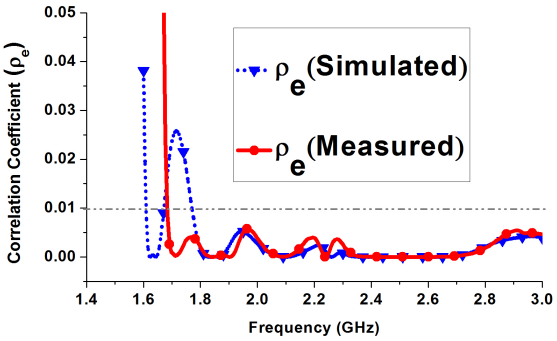

Figure 9. Correlation of the proposed MIMO antenna

B. *Mean Effective Gain (MEG) and Diversity Gain (DG)*

In the case of mobile wireless environment for a series of assumptions [10], the MEGs can be calculated by Eq. (2). The MEGs obtained from measured radiation data are listed in Table II. It is found that the MEG for each antenna element is almost identical. In worst case situation, the maximum ratio of the MEG between any of the two antenna units is not more than 1.7 dB. Therefore, the received signals satisfy the conditions $P_i \approx P_j$ ($|MEG_i/MEG_j| < 3$ dB) [11].

$$MEG_i = \frac{1}{2\pi} \times \left[\int_0^{2\pi} \left[\frac{\Gamma}{1+\Gamma} G_{\theta i}\left(\frac{\pi}{2}, \varphi\right) + \frac{1}{1+\Gamma} G_{\varphi i}\left(\frac{\pi}{2}, \varphi\right) \right] d\varphi \right] \quad (2)$$

Where $G_{\theta i}(\Omega)$ and $G_{\varphi i}(\Omega)$ are the power gain patterns of *i*th antenna, and Γ represents the cross polarization discrimination; assuming Γ= 0 dB in indoor fading environment [11].

TABLE II
MEAN EFFECTIVE GAIN AND DIVERSITY GAIN FOR THE PROTOTYPE

Center Frequency (GHz)	Mean Effective Gain in dB (Indoor, Γ = 0 dB)		K (dB)	DG, 1% (dB)
	Ant. #1	Ant. #2		
1.80	-17.50	-17.46	0.04	9.95
1.92	-22.49	24.18	1.69	8.30
2.10	-09.83	-08.52	1.31	8.68
2.35	-08.78	-08.33	0.44	9.56
2.45	-09.42	-08.73	0.69	9.31
2.60	-11.54	-10.73	0.81	9.19

Under the selected combining scheme and at 99% link reliability, the computed diversity gain (DG) by using Eq. (3) [12], which are obtained from the measured data, are presented in Table II. The high diversity gains are obtained over the operating bands.

$$DG = DG_0 \cdot \left(\sqrt{1-\rho_{ij}^{e}}\right) \cdot K \tag{3}$$

$$K = \min\left(\frac{MEG_1}{MEG_2}, \frac{MEG_2}{MEG_1}\right) \tag{4}$$

Where, DG_0 = 10 dB [12] represents the ideal diversity gain of the antenna.

C. Radiation Characteristics

The measured 2D radiation patterns of the proposed MIMO antenna at 2.5 GHz frequency are plotted in Fig. 10. It is observed that the radiation pattern is almost omnidirectional and tends to cover the complementary space region. This approach can overcome the multipath fading problems and enhance the systems performance.

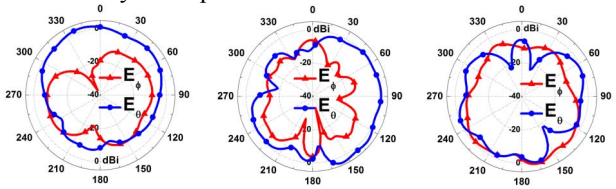

(a) x-y plane (b) x-z plane (c) y-z plane

At Antenna Unit 1

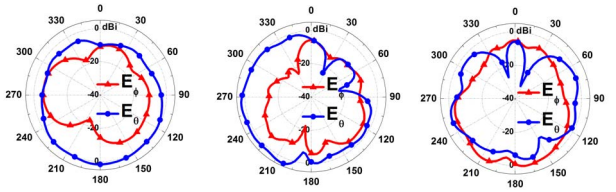

(d) x-y plane (e) x-z plane (f) y-z plane

At Antenna Unit 2

Figure 10. Measured 2D radiation patterns at 2.5 GHz

IV. CONCLUSION

A printed broadband MIMO antenna system is presented. At VSWR ≤ 2.75, the measured bandwidths are around 530 MHz and 670 MHz, respectively. The applied decoupling techniques work effectively and hence high isolation (> 18 dB) is achieved. The MEGs, DGs and correlation coefficients are computed from the measured far-field radiation patterns and ensuring high diversity performance. The proposed MIMO antenna occupies total size of 60×110×0.8mm^3, which is a typical mobile handset's size for practical usage and comparable with the IPhone4 mobile handset. Moreover, a footprint of each single antenna unit is only 15×18.5mm^2, which makes it fit for antenna array.

ACKNOWLEDGMENT

The author would like to thank the Key Laboratory of Autonomous Systems and Networked Control, SCUT, Ministry of Education, Guangzhou. The work was partially supported by the Funds for Natural Science Foundation of China under Grant 61074097 and Project on the Integration of Industry, Education and Research of Guangdong Province (2012B091100039).

REFERENCES

[1] C. E. Shannon, "A mathematical theory of communication," *Bell Syst. Tech. J.,* vol. 27, pp. 379-423, Jul. 1948.

[2] E. Dahlman, S. Parkvall, J. Skold, and P. Beming, *3G Evolution: HSPA and LTE for Mobile Broadband,* 2nd ed., Academic Press, Oxford, 2007.

[3] G. J. Foschini and M. J. Gans, "On limits of wireless communications in a fading environment when using multiple antennas," *Wireless Pres. Commun.,* vol. 6, no. 3, pp. 331-335, 1998.

[4] S. H. Chan, R. A. Abd-Alhameed, Z. Z. Abidin, N. J. McEwan, and P. S. Excell, "Wideband printed MIMO/Diversity monopole antenna for WiFi/WiMAX Applications," *IEEE Trans. Antennas Propag.,* vol. 60, no. 4, pp. 3936-3939, Apr. 2012.

[5] C.-C. Hsu, K. –H. Lin, and H.-L. Su, "Implementation of Broadband Isolator Using Metamaterial-Inspired Resonators and a T-Shaped Branch for MIMO Antennas," *IEEE Trans. Antennas Propag.,* vol. 59, no. 10, pp. 3936-3939, Oct. 2011.

[6] J. Li, Q. Chu, and T. Huang, "A compact wideband MIMO antenna with two novel bent slits," *IEEE Trans. Antennas Propag.,* vol. 60, no. 2, pp. 482-489, Feb. 2012.

[7] D. Shen, T. Guo, F. Kuang, X. Zhang, and D. Wu, " A novel wideband printed diversity antenna for mobile handsets," in *Proc. IEEE Vehicular Technology Conference (75th VTC Spring),*pp. 1-5, May. 2012.

[8] C. H. Chang and K. Wong, "Printed λ/8-PIFA for Penta-Band WWAN Operation in the Mobile Phone," *IEEE Trans. Antennas Propag.,* vol. 57, no. 5, pp. 1337-1381, May. 2009.

[9] H. Paul, "The significance of radiation efficiencies when using s-parameters to calculate the received signal correlation form two antennas," *IEEE Antennas Wireless Propag. Lett.,* vol. 4, no. 1, pp. 97-99, Jun. 2005.

[10] S. C. K. Ko and R. D. Murch, "Compact integrated diversity antenna for wireless communications," *IEEE Trans. Antennas Propag.* Vol. 49, pp. 954-960, Jun. 2001.

[11] R. G. Vaughan and J. B. Anderson, "Antenna diversity in mobile communications," *IEEE Trans. Veh. Technol.,* vol. 36, pp. 147-172, Nov. 1987.

[12] Y. Gao, X. D. Chen, and Z. N. Ying, "Design and performance investigation of a dual-element PIFA array at 2.5 GHz for MIMO terminal," *IEEE Trans. Antennas Propag.,* vol. 55, no. 12, pp. 3433-3441, Jun. 2007.